MODELING THE DAMAGE BEHAVIOR OF SUPERPLASTIC MATERIALS

Di Gioacchino, Fabio
Soldà, Alessandro
Minak, G. , giangiacomo.minak@unibo.it
DIEM, Facoltà di Ingegneria, Università degli Studi di Bologna via Risorgimento, 2 – 40136 Bologna, Italia

Costa-Mattos, H. S., heraldo@mec.uff.br
PGMEC, Laboratório de Mecânica Teórica e Aplicada,Universidade Federal Fluminense , Rua Passo da Patria 156 , 24210-240, Niterói, RJ, Brazil

Abstract. *The present paper is concerned with the modeling of superplasticity phenomenon in metallic materials using a continuum damage theory. The goal is to propose a one-dimensional phenomenological damage model, as simple as possible, able to perform a mathematically correct and physically realistic description of plastic deformations, strain hardening, strain softening, strain rate sensitivity and damage (nucleation and growth of voids) observed in tensile tests performed at different strain rates. Examples concerning the modeling of tensile tests of a magnesium alloy at different strain rates are presented and analyzed. The results obtained show a very good agreement between experimental results and model prevision*

Keywords*: superplasticity, tensile tests, strain rate sensitivity, continuum damage mechanics*

1. INTRODUCTION

A wide class of materials - metals, ceramics, intermetalics, nanocrystaline, etc - show superplastic behavior under special processing conditions. Although, up to now, there is no precise physical definition of superplasticity phenomenon in metallic materials, from a phenomenological point of view, superplasticity can be defined as very high deformations prior to local failure. In the case of tensile tests under controlled strain rate, this means very high elongations of the specimens before rupture. The deformation process is generally conducted at high temperature and the strain can be 10 times the obtained under room temperature. Superplastically deformed material in tensile tests gets thinner in a very uniform manner, rather than forming a 'neck' (a local narrowing) which leads to fracture.

The most important characteristic of a superplastic material is its high strain rate sensitivity of flow stress that confers a high resistance to neck development and results in the high tensile elongations characteristic of superplastic behavior. Superplasticity is used to form directly complex objects, by the application of gas pressure or with a tool, and often with the help of dies, avoiding complicated and costly joining and machine steps. The applications of superplastic formations were originally limited to the aerospace industry, but it has recently been expanded to include the automobile industries as a result of breakthroughs in the range of materials that can be made superplastic and the rate at which the phenomenon takes place.

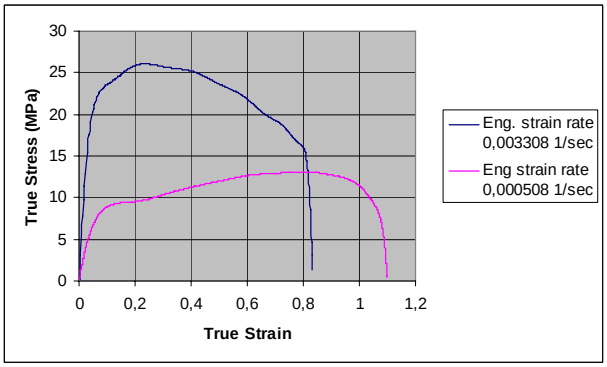

Figure 1: Strain hardening, strain softening, strain rate sensitivity and damage in AZ31B-F magnesium alloy at 400 ^{0}c

The present paper is concerned with the modeling of such phenomenological behavior using a continuum damage theory. Most of the studies presented up to now in the literature are concerned with micro-structural aspects of the phenomenon. It is not the goal here to discuss the microscopic mechanisms of superplastic deformation. In the case of superplasticity, the damage is mainly due to nucleation and growth of voids in the material. An interesting analysis of cavity initiation and growth can be found in Khaleel et al, 2001. Other experimental works about superplastic behavior

in magnesium alloys can be found in Kim et al 2001; Xin Wu and Yi Liu., 2002; Tan, 2002 ; Somekawa et al, 2003; Lin et al, 2005; Takuda et al, 2005; Yin, $2005_{a,b}$; Lee, et al, 2005. The goal of the present paper is to propose a one-dimensional phenomenological damage model, as simple as possible, able to perform a mathematically correct and physically realistic description of plastic deformations, strain-hardening, strain-softening, strain rate sensitivity and damage observed in tensile tests performed at different strain rates and temperatures. Besides, the experimental identification of the parameters that appear in the model must also be as simple as possible. The identification of parameters that appear in the theory is discussed in detail and examples concerning the modeling of tensile tests of a magnesium alloy at different strain rates and temperatures is presented and analyzed. The results obtained show a very good agreement between experimental results and model prevision.

2. BASIC DEFINITIONS

Let's consider a simple tension test in which the specimen has a gauge length L and cross section A_o submitted to a prescribed elongation $F(t)$. The force necessary to impose such elongation is noted F

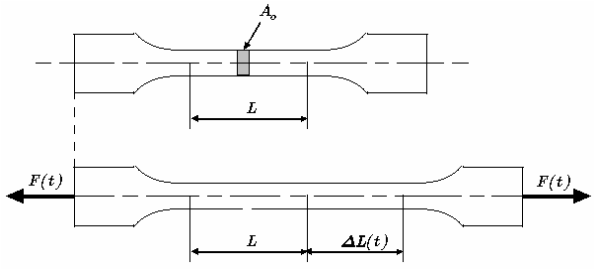

Figure 2: Specimen for a tension test

The so-called engineering strain ε and the engineering stress σ are defined as

$$\varepsilon(t) = \frac{\Delta L(t)}{L} \quad ; \quad \sigma(t) = \frac{F(t)}{A_o} \tag{1}$$

The so-called true strain ε_t and true stress σ_t are defined as

$$\varepsilon_t = ln(1+\varepsilon) \quad ; \quad \sigma_t = \sigma(1+\varepsilon) \tag{2}$$

From definitions (1) and (2) it is possible to obtain the following relations

$$\varepsilon_t = ln(1+\varepsilon) \Rightarrow exp(\varepsilon_t) = exp(ln(1+\varepsilon)) \Rightarrow \varepsilon = exp(\varepsilon_t) - 1 \Rightarrow$$
$$\dot{\varepsilon} = exp(\varepsilon_t)\,\dot{\varepsilon}_t \quad ; \quad \dot{\varepsilon}_t = \frac{\dot{\varepsilon}}{(1+\varepsilon)} \tag{3}$$

The ASTM Standard E 2448 – 05 "Standard Test Method for Determining the Superplastic Properties of Metallic Sheet Materials" describes the procedure for determining the superplastic forming properties (SPF) of a metallic sheet material. It includes tests both for the basic SPF properties and also for derived SPF properties. The test for basic properties encompasses effects due to strain hardening or softening.

3. MODELING THE TRUE STRESS X TRUE STRAIN CURVE WITHOUT DAMAGE (BEFORE SOFTENING)

HIP 1: $\sigma_t = a\,\left[1 - exp(-b\varepsilon_t)\right]$, with a and b being positive functions of ε_t and $\dot{\varepsilon}_t$

CHOICE : $a(\varepsilon_t, \dot{\varepsilon}_t) = K_a\left[\dot{\varepsilon}_t\, exp(\varepsilon_t)\right]^{N_a}$, $ab(\varepsilon_t, \dot{\varepsilon}_t) = K_{ab}\, ln\left[\dot{\varepsilon}_t\, exp(\varepsilon_t)\right] + N_{ab}$ with K_a, N_a, K_{ab} and N_{ab} being temperature dependent positive parameters. Since $\dot{\varepsilon} = \dot{\varepsilon}_t\, exp(\varepsilon_t)$, a and b are constants in tensile tests with fixed value of the engineering strain rate $\dot{\varepsilon}$. Hence,

$$\Rightarrow a = K_a\,[\dot{\varepsilon}]^{N_a} \quad , \quad ab = K_{ab}\, ln(\dot{\varepsilon}) + N_{ab} \tag{4}$$

If $N_a = 0$ the parameter a is independent of the strain rate $\dot{\varepsilon} \Rightarrow a = K_a$
If $N_b \to \infty$ the parameter ab is independent of the strain rate $\dot{\varepsilon} \Rightarrow ab \to \infty$

3.1. Parameters identification

3.1.1. Preliminary definitions

All parameters K_a, N_a, K_{ab}, N_{ab} can be identified from two tensile tests with constant engineering strain rates $\dot{\varepsilon}_1$ and $\dot{\varepsilon}_2$. In a tensile test with constant engineering stress rate $\dot{\varepsilon}_i$, the true stress σ_t can be expressed as

$$\sigma_t = a_i \left[1 - exp(-b_i \varepsilon_t)\right] \tag{5}$$

with

$$a_i = K_a \left[\frac{exp(\varepsilon_t)\ \dot{\varepsilon}_t}{\dot{\varepsilon}_i}\right]^{N_a} \quad , \quad a_i b_i = K_{ab}\, ln\left(\frac{exp(\varepsilon_t)\ \dot{\varepsilon}_t}{\dot{\varepsilon}_i}\right) + N_{ab} \tag{6}$$

The parameters a_i and b_i can be identified from the true stress X true strain curve obtained in a tensile test with constant engineering strain rate $\dot{\varepsilon}$ using a minimum squares curve fitting technique or using the following simpler procedure:

3.1.2. Identification of a_i

The parameter a_i can be identified from the true stress X true strain curve. From (5), it is possible to obtain:

$$\lim_{\varepsilon_i \to \infty} (\sigma_t) = a_i \tag{7}$$

Hence, a_i is the maximum value of the stress σ_t

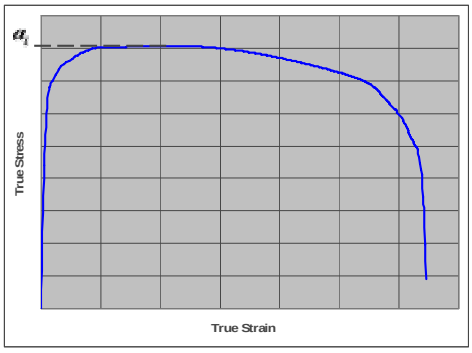

Figure 3: Identification of the parameter a_i from the true stress X true strain curve.

3.1.3. Identification of b_i

From (5) it is also possible to verify that $\left.\frac{d\sigma_t}{d\varepsilon_t}\right|_{\varepsilon_t = 0} = a_i b_i$

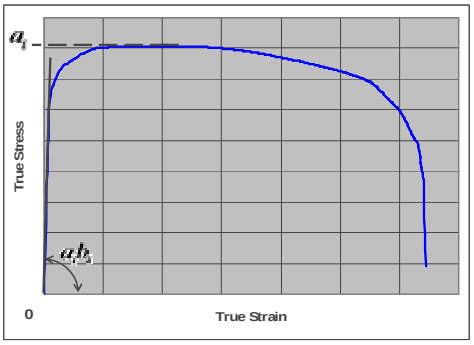

Figure 4: Identification of the parameter b_i from the true stress X true strain curve

Hence, once a_i is known, b_i can be identified from the initial slope of the true stress X true strain curve. From (2) it is possible to obtain

$$exp(-b_i\varepsilon_t) = \left(\frac{a_i - \sigma_t}{a_i}\right) \quad \text{or,} \quad -b_i\varepsilon_t = ln\left(\frac{a_i - \sigma_t}{a_i}\right)$$

And b_i can be approximated from the following expression:

$$b_i = -\left(\frac{1}{\varepsilon_t}\right) ln\left(\frac{a_i - \sigma_t}{a_i}\right) \tag{8}$$

3.1.4. Identification of K_a, N_a, K_b, N_b

Once a_1, b_1 and a_2, b_2 are identified from two tensile tests with different engineering strain rates $\dot{\varepsilon}_1$ and $\dot{\varepsilon}_2$, the parameters K_a, N_a, K_b, N_b can also be identified.

From (6) it is possible to obtain

$$ln(K_a) + N_a\, ln(\dot{\varepsilon}_1) = ln(a_1) \tag{9}$$

and

$$-\left[ln(K_a) + N_a\, ln(\dot{\varepsilon}_2) = ln(a_2)\right] \tag{10}$$

Combining these equations it is possible to obtain

$$N_a\left[ln(\dot{\varepsilon}_1) - ln(\dot{\varepsilon}_2)\right] = \left[ln(a_1) - ln(a_2)\right] \Rightarrow N_a = \frac{\left[ln(a_1) - ln(a_2)\right]}{\left[ln(\dot{\varepsilon}_1) - ln(\dot{\varepsilon}_2)\right]} \tag{11}$$

The parameter K_a can be obtained from the following equation

$$K_a = \frac{a_1}{(\dot{\varepsilon}_1)^{N_a}} \tag{12}$$

With a similar procedure it is possible to verify that

$$a_1b_1 - K_{ab}ln(\dot{\varepsilon}_1) = N_{ab} \tag{13}$$

and

$$-[a_2b_2 - K_{ab}ln(\dot{\varepsilon}_2) = N_{ab}] \tag{14}$$

Combining these equations it is possible to obtain

$$a_1b_1 - a_2b_2 = K_{ab}[ln(\dot{\varepsilon}_1) - ln(\dot{\varepsilon}_2)] \Rightarrow K_{ab} = \frac{a_1b_1 - a_2b_2}{ln(\dot{\varepsilon}_1) - ln(\dot{\varepsilon}_2)} \tag{15}$$

The parameter N_{ab} can be obtained from the following equation

$$N_{ab} = a_1b_1 - K_{ab}ln(\dot{\varepsilon}_1) \tag{16}$$

Finally, from (6) it is possible to predict the values of a_ib_i, a_i for tensile test at different strain rates and calculate b_i as a_ib_i and a_i ratio.

$$b_i = \frac{a_i b_i}{a_i} \Rightarrow b_i = \frac{K_{ab}\, ln(\dot{\varepsilon}) + N_{ab}}{K_a\, [\dot{\varepsilon}]^{N_a}} \tag{17}$$

The typical trend of the b *vs* $\dot{\varepsilon}$ curve is shown in Fig. 5 below

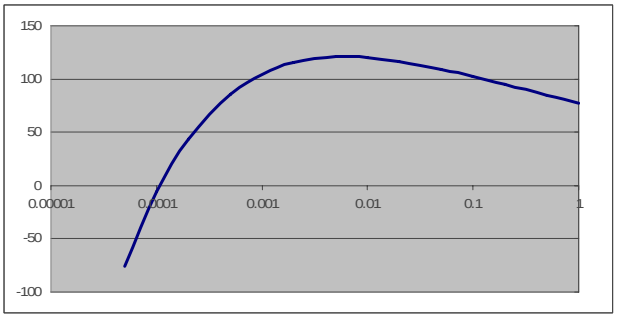

Figure 5: Variation of coefficient b for tensile tests at different strain rates

3.2. Example: magnesium alloy AZ31B-F at 375 ^{0}C

The experimental results considered on this paper are taken from Del Valle, 2005. The Chemical Composition is presented at this reference

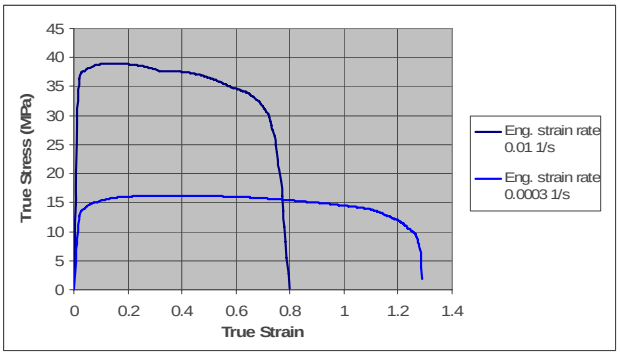

Figure 5: Magnesium alloy AZ31B-F at 375 ^{o}C. Two different strain rates $\dot{\varepsilon}_1 = 0,0003\ (1/sec)$ and $\dot{\varepsilon}_2 = 0,01\ (1/sec)$

For two different engineering strain rates $\dot{\varepsilon}_1 = 0,0003\ (1/sec)$ and $\dot{\varepsilon}_2 = 0,01\ (1/sec)$ we have $a_1 = 16,15\ MPa$; $a_1 b_1 = 1130,5\ MPa$; $a_2 = 38,99\ MPa$; $a_2 b_2 = 5068,7\ MPa$

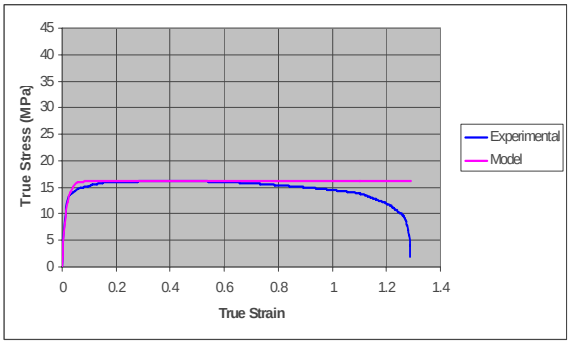

Figure 6: Stress-strain curve for $\dot{\varepsilon}_1 = 0,0003\ (1/sec)$

From (11), (12), (15) and (16) it is possible to obtain $N_a = 0,251$; $K_a = 124,06\ MPa$; $N_{ab} = 68.98$; $K_{ab} = 6,51\ MPa$

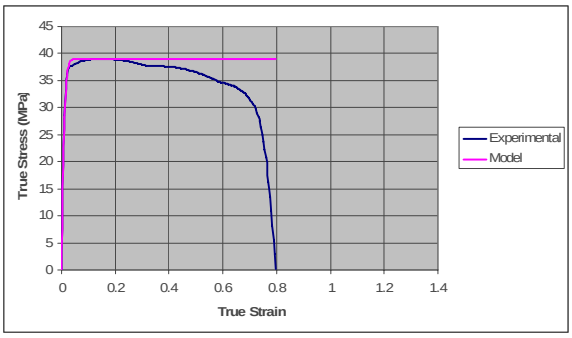

Figure 7: Stress-strain curve for $\dot{\varepsilon}_2 = 0,01\ (1/sec)$

4. MODELING THE TRUE STRESS X TRUE STRAIN CURVE WITH DAMAGE

Only a few damage models were proposed for superplastic alloys, such as Chandra, 2002. In the present paper it is introduced an auxiliary variable D that accounts for the nucleation and growth of voids observed in tensile tests performed at different strain rates.

HIP 2: $\sigma_t = (1 - D)\ a\ [1 - exp(-b\varepsilon_t)]$ $\quad with \quad$ $0 \leq D \leq 1$ $\quad and$

$$a_d = K_{a_d}[\dot{\varepsilon}]^{-N_{a_d}}\ ,\ if\ \dot{\varepsilon} > 0.1\ seg^{-1} \quad or \quad (\ a_d = -K_{a_d}(\dot{\varepsilon}) + N_{a_d}\ ,\ if\ \dot{\varepsilon} \leq 0.1\ seg^{-1})$$

$$a_d b_d = K_{a_d b_d}[\dot{\varepsilon}]^{-N_{a_d b_d}}$$

HIP 3: $$D = \begin{cases} 0, \ if\ AUX > 1 \\ -\left[\frac{1}{b_d}\right] ln(AUX), \ if\ 0 < AUX < 1 \\ 1, \ if\ AUX < 0 \end{cases} \quad with \quad AUX = 1 - \left(\frac{\varepsilon_t - K_d/b}{a_d}\right)$$

Where a_d, b_d, and K_d are temperature dependent positive parameters.

4.1. Parameters identification

4.1.1. Preliminary definitions

All parameters K_d, N_d, a_d, b_d can be identified from two tensile tests with constant engineering strain rates $\dot{\varepsilon}_1$ and $\dot{\varepsilon}_2$. Considering HIP 2. For a tensile test with constant stress rate $\dot{\varepsilon}_i$, the damage variable D can be expressed as $\frac{\sigma_t}{a\left[1-exp(-b\varepsilon_t)\right]} = (1 - D) \Rightarrow D = 1 - \frac{\sigma_t}{a\left[1-exp(-b\varepsilon_t)\right]}$, after the softening behavior. Hence, the experimental curve $D \times \varepsilon_t$ can be easily obtained.

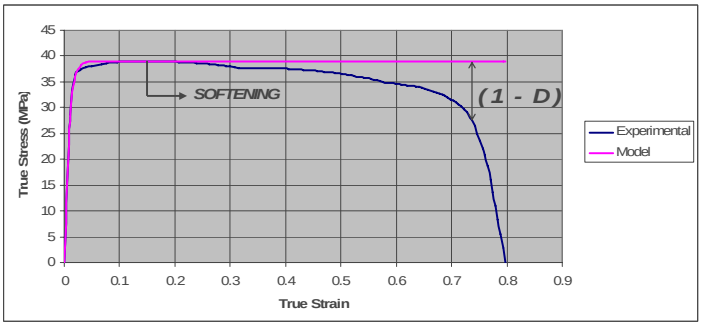

Figure 8: Experimental identification of the auxiliary variable D.

Since $\dot{\varepsilon} = exp(\varepsilon_t)\ \dot{\varepsilon}_t$, it is possible to obtain from HIP 3

$$D = -\left[\frac{1}{b_d}\right] \ln\left[1 - \left\langle \frac{\varepsilon_t - K_d/b}{a_d} \right\rangle\right], \text{ for } D \in [0,1) \Rightarrow$$

$$-b_d D = \ln\left[1 - \left\langle \frac{\varepsilon_t - K_d/b}{a_d} \right\rangle\right], \text{ for } D \in [0,1) \Rightarrow$$

$$\exp(-b_d D) = 1 - \left\langle \frac{\varepsilon_t - K_d/b}{a_d} \right\rangle, \text{ for } D \in [0,1) \Rightarrow$$

$$\left\langle \frac{\varepsilon_t - K_d/b}{a_d} \right\rangle = 1 - \exp(-b_d D), \text{ for } D \in [0,1) \Rightarrow$$

$$\langle \varepsilon_t - K_d/b \rangle = a_d [1 - \exp(-b_d D)], \text{ for } D \in [0,1) \Rightarrow$$

$$\varepsilon_t = a_d [1 - \exp(-b_d D)] + K_d/b \tag{18}$$

The parameter a_i and b_i can be identified from the true stress X true strain curve obtained in a tensile test with constant engineering strain rate $\dot{\varepsilon}$. using a minimum squares curve fitting technique or using the following simpler procedure. If $D = 0$, from (11) it is possible to obtain

$$\varepsilon_t = \frac{K_d}{b}$$

A "corrected curve" is obtained by eliminating the viscous term K_d/b from this curve.

$$(\varepsilon_t)_{corrected} = a_d [1 - \exp(-b_d D)] \tag{19}$$

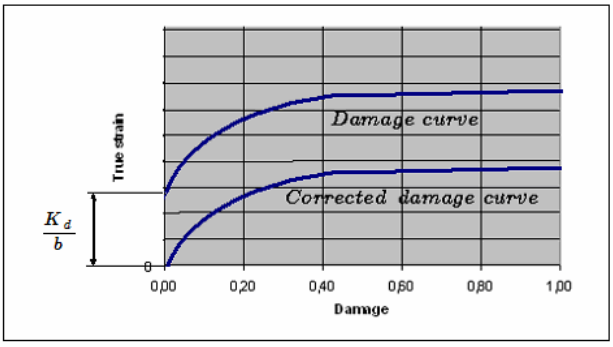

Figure 9: Damage curve and corrected damage curve obtained from a tensile test with constant engineering stress rate.

The parameters a_i and b_i can be identified from the true stress X true strain curve using a minimum squares curve fitting technique or using the following simpler procedure.

4.1.2. Identification of a_d

From (18), it is possible to obtain:

$$\lim_{D \to 1}((\varepsilon_t)_{corrected}) = a_d \tag{20}$$

Hence, a_d is the value of the corrected strain $(\varepsilon_t)_{corrected}$ when $D \to 1$

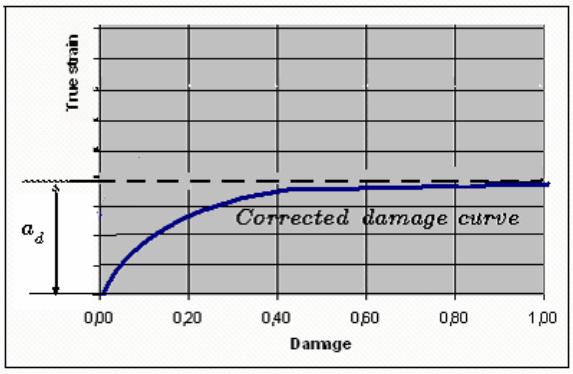

Figure 10: Experimental identification of a_d.

4.1.3. Identification of b_d

From (18) it is possible to verify that

$$\left.\frac{d(\varepsilon_t)_{corrected}}{dD}\right|_{D=0} = a_d b_d$$

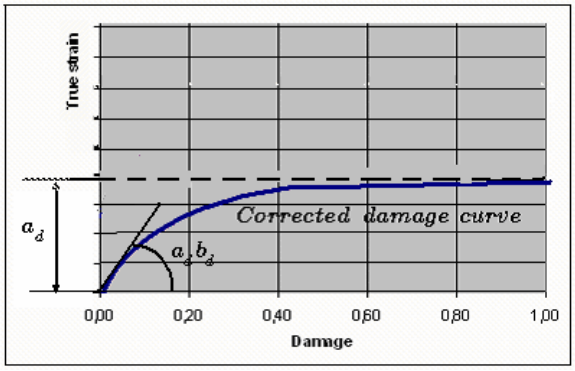

Figure 11: Identification of the parameter b_i from the true stress X true strain curve

Hence, once a_d is known, b_d can be identified from the initial slope of the true corrected damage curve. From (18) it is possible to obtain

$$exp(-b_d D) = \left(\frac{a_d - (\varepsilon_t)_{corrected}}{a_d}\right) \quad \text{or,} \quad -b_d D = ln\left(\frac{a_d - (\varepsilon_t)_{corrected}}{a_d}\right)$$

b_d can be approximated from the following expression:

$$b_d = -\left(\frac{1}{D}\right) ln\left(\frac{a_d - (\varepsilon_t)_{corrected}}{a_d}\right) \tag{21}$$

4.1.4. Identification of K_d

Once the parameters the parameters a_d and b_d are obtained, the parameter K_d can be identified from the strain *vs* damage curves obtained in a tensile test with constant strain rates $\dot{\varepsilon}_1$. and $\dot{\varepsilon}_2$. The value η

$$\eta = \frac{K_d}{b}$$

can be obtained from both experimental damage curves, considering an avarage value. Hence, we have

$$K_d = \frac{b_1\eta_1 + b_2\eta_2}{2} \qquad and \qquad \eta_i = \frac{K_d}{b_i} \tag{22}$$

4.2. Example: magnesium alloy AZ31B-F at 375 ^{0}c

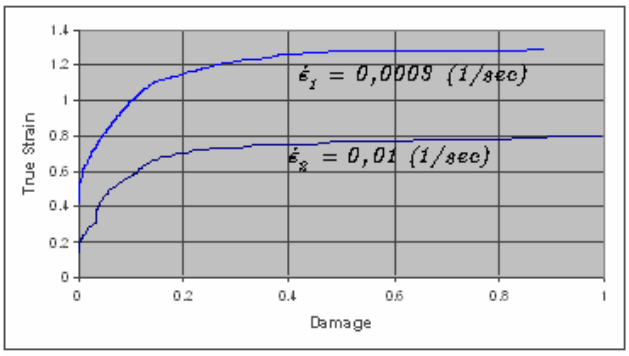

Figure 12: Damage curves for $\dot{\varepsilon}_1 = 0{,}0003\ (1/sec)$ and $\dot{\varepsilon}_2 = 0{,}01\ (1/sec)$

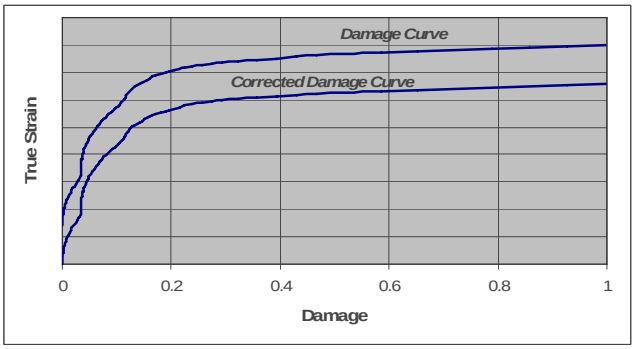

Figure 13: Corrected curve obtained for $\dot{\varepsilon}_2 = 0{,}01\ (1/sec)$

For the two considered strain rates we have: $a_{d_1} = 1{,}12$; $a_{d_1}b_{d_1} = 13{,}44$; $a_{d_2} = 0{,}72$, $a_{d_2}b_{d_2} = 7{,}92$

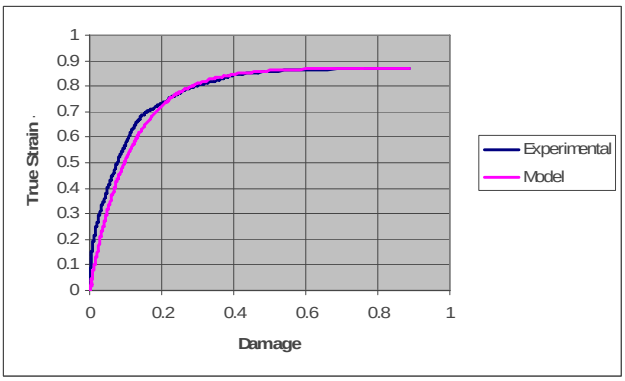

Figure 14: Corrected damage curve. Model and experiment. $\dot{\varepsilon}_1 = 0{,}003\ (1/sec)$.

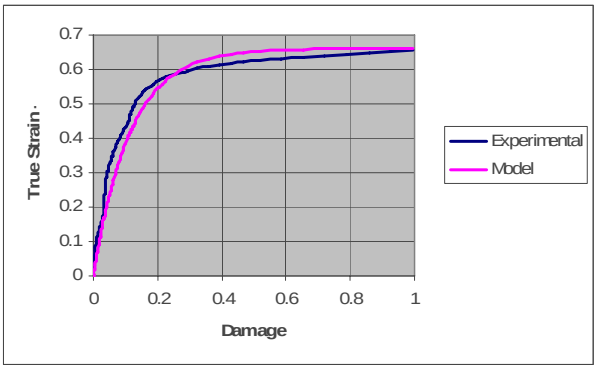

Figure 15: Corrected damage curve. Model and experiment. $\dot{\varepsilon}_2 = 0,01\ (1/sec)$.

Once the parameters the parameters a_d and b_d are obtained, the parameter K_d can be identified from the strain *vs* damage curves obtained in a tensile test with constant strain rates $\dot{\varepsilon}_1$ and $\dot{\varepsilon}_2$. Since

$$\eta_1 = 0,067 = (\varepsilon_{max})_{curve1} - a_d \quad ; \quad \eta_2 = 0,12 = (\varepsilon_{max})_{curve2} - a_d$$

hence, from (22) we have $K_d = 8,71$

IV- PROPOSED MODEL

$$\sigma_t = (1 - D)\ a\ \left[1 - exp\left(-b\varepsilon_t\right)\ \right]$$

with

$$a_d = K_{a_d}\,[\dot{\varepsilon}]^{-N_{a_d}} \quad or \quad (\ a_d = -K_{a_d}(\dot{\varepsilon}) + N_{a_d}\ )\ , \qquad a_d b_d = K_{a_d b_d}\,[\dot{\varepsilon}]^{-N_{a_d b_d}}$$

$$D = \begin{cases} 0, & if\ AUX > 1 \\ -\left[\dfrac{1}{b_d}\right]\ ln(AUX), & if\ 0 < AUX < 1 \\ 1, & if\ AUX < 0 \end{cases}$$

$$AUX = 1 - \left(\frac{\varepsilon_t\ -\ [K_d\ /\ b]}{a_d}\right)$$

The following coefficients were identified for the magnesium alloy AZ31B-F: $a_1 = 16,15\ MPa$; $a_1 b_1 = 1130,5\ MPa$; $a_2 = 38,99\ MPa$; $a_2 b_2 = 5068,7\ MPa$; $N_a = 0,251$; $K_a = 124,06\ MPa$; $N_{ab} = 68.98$; $K_{ab} = 6,51\ MPa$; $a_{d_1} = 1,15$; $a_{d_1} b_{d_1} = 13,44$; $a_{d_2} = 0,73$; $a_{d_2} b_{d_2} = 7,92$; $K_d = 8,71$.

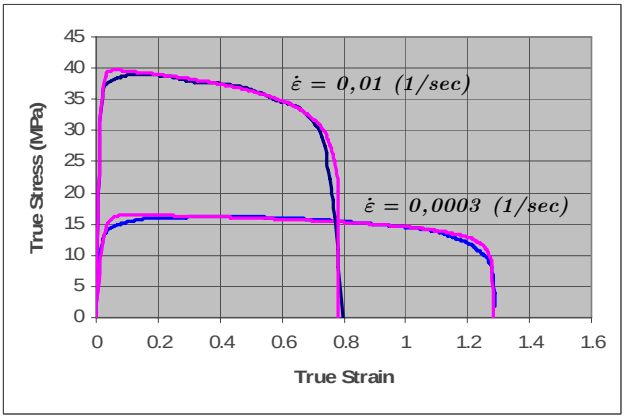

Figure 16: Stress-strain curve for $\dot{\varepsilon}_1 = 0,0003\ (1/sec)$ and $\dot{\varepsilon}_2 = 0,01\ (1/sec)$

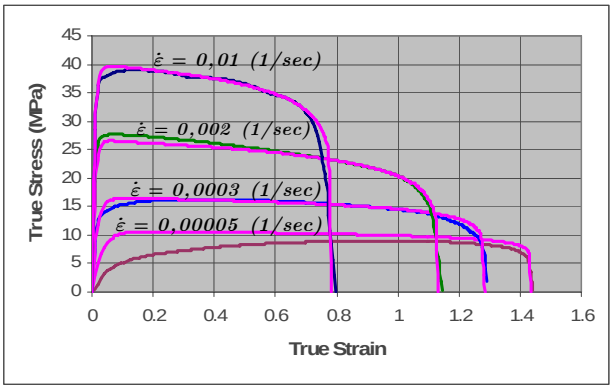

Figure 17: Stress-strain curve for different engineering strain rates.

Furthermore, good predictions have been obtained considering the experimental results from Xin Wu 2001, referred to tensile tests carried out at 500 °C on AZ31 magnesium alloy.

The following coefficients were identified: $a_1 = 25,2\ MPa$; $a_1 b_1 = 1366,3\ MPa$; $a_2 = 63,8\ MPa$; $a_2 b_2 = 1480,1\ MPa$; $N_a = 0,2017$; $K_a = 63,8\ MPa$; $N_{ab} = 1480.2$; $K_{ab} = 24,71\ MPa$; $a_{d_1} = 1,2$; $a_{d_1} b_{d_1} = 3,42$; $a_{d_2} = 0,34$; $a_{d_2} b_{d_2} = 1,19$; $K_d = 7,23$.

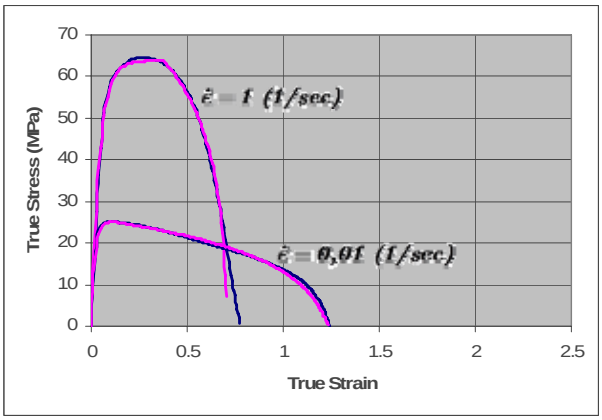

Figure 18: Stress-strain curve for $\dot{\varepsilon}_1 = 0,01\ (1/sec)$ and $\dot{\varepsilon}_2 = 1\ (1/sec)$ from Xin Wu 2001

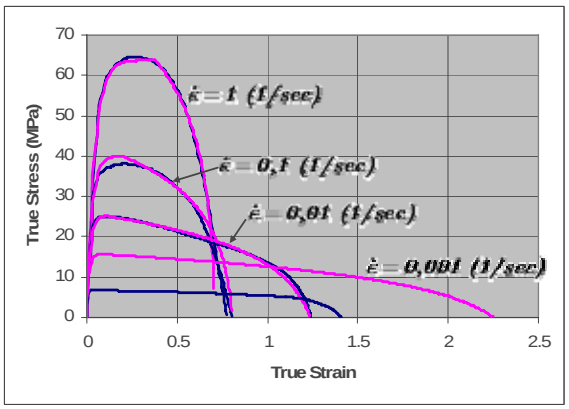

Figure 19: Stress-strain curve for different engineering strain rates

5. CONCLUDING REMARKS

The one-dimensional phenomenological damage model proposed on this paper is able to perform a mathematically correct and physically realistic description of plastic deformations, strain hardening, strain softening,

strain rate sensitivity and damage observed in tensile tests performed at different strain rates and temperatures. The identification of parameters that appear in the theory is discussed in detail and examples concerning the modeling of tensile tests of a magnesium alloy at different strain rates and temperatures are presented and analyzed. It is necessary to perform only two tensile tests at different strain rates in order to identify the parameters that appear in the theory. The results obtained show a very good agreement between experimental results and model prevision for different strain rates. Finally, it is important to observe that it is necessary to adapt such model to account for compression loading, what can be done through the introduction of a new auxiliary variable related to the cumulated plastic strain. It is also necessary an adequate thermo mechanical framework in order to extend the proposed model to a tri-dimensional context, which is essential since one of the main practical motivation to study such alloys is the superplastic forming (SPF) of sheet metals. In a tri-dimensional context, the adequate choice of the measure of strain and of the objective time derivative is essential to built a physically realistic and mathematically correct model (Costa-Mattos, 1998).

6. REFERENCES

ASTM Standard E 2448 – 05. "Standard Test Method for Determining the Superplastic Properties of Metallic Sheet Materials".

B.H. Lee, K. S. Shin and C. S. Lee. "High temperature Behavior of AZ31 Mg Alloy". Materials Science Forum Vols 475-479 (2005) pp. 2927-2950

Chandra, N. "Constitutive behavior of superplastic materials". International Journal of Non-Linear Mechanics 37 (2002) 461-484

Costa-Mattos, H. "A Thermodynamically Consistent Constitutive Theory for Fluids". International Journal of Non-linear Mechanics. Vol. 33, no. 1 (1998), pp. 97 - 110

D.L. Yin, K. F. Zang, G. F. Wang. "Microstructure evolution and fracture behavior in superplastic deformation of hot-holled AZ31 Mg alloy sheet". Materials Science Forum Vols 475-479 (2005) pp. 2923-2926

D.L. Yin, K.F. Zhang, G.F. Wang, W.B. Han, "Superplasticity and cavitation in AZ31 Mg alloy at elevated temperatures". Materials Letters 59 (2005) 1714– 1718

H. Takuda, T. Morishita, T. Kinoshita, N. Shirakawa. "Modelling of formula for flow stress of a magnesium alloy AZ31 sheet at elevated temperatures". Journal of Materials Processing Technology 164–165 (2005) 1258–1262

J.A. Del Valle, M.T. PéreZ-Prado, and O.A. Ruano. "Deformation mechanisms responsible for the high ductility in a Mg AZ31 alloy analyzed by electron backscattered diffraction". Metallurgical And Materials Transactions A 1427-1438—Volume 36A, June 2005.

J.C. Tan, M.J. Tan. "Superplasticity in a rolled Mg–3Al–1Zn alloy by two-stage deformation method". Scripta Materialia 47 (2002) 101–106

Lin, H.K., J.C. Huang, T.G. Langdon. "Relationship between texture and low temperature superplasticity in an extruded AZ31 Mg alloy processed by ECAP". Materials Science and Engineering A 402 (2005) 250–257

M.A. Khaleel, H.M. Zbib, E.A. Nyberg. "Constitutive modeling of deformation and damage in superplastic materials" International Journal of Plasticity 17 (2001) 277-296

Somekawa, H., Hosokawa, H., Watanabe, H. and Higashi, K. "Diffusion bonding in superplastic magnesium alloys". Materials Science and Engineering A339 (2003) 328_/333

W. J. Kim, S. W. Chung, C. S. Chung and D. Kum. "Superplasticity in thin magnesium alloy sheets and deformation mechanism maps for magnesium alloys at elevated temperatures". Acta Mater. 49 (2001) 3337–3345.

Xin Wu, Yi Liu. "Superplasticity of coarse-grained magnesium alloy". Scripta Materialia 46 (2002) 269–274

7. RESPONSIBILITY NOTICE

The author(s) is (are) the only responsible for the printed material included in this paper.